

Characterization of a Single Molecule DNA Switch in Free Solution

Samuel S. White,[†] Haitao Li,[†] Richard J. Marsh,[‡] Joe D. Piper,[†]
Nicholas D. Leonczek,[‡] Nick Nicolaou,[‡] Angus J. Bain,[‡] Liming Ying,^{*,†} and
David Klenerman^{*,†}

Contribution from the Department of Chemistry, University of Cambridge, Lensfield Road, Cambridge CB2 1EW, and Department of Physics and Astronomy, University College London, Gower Street, London WC1E 6BT

Received March 3, 2006; E-mail: ly206@cam.ac.uk; dk10012@cam.ac.uk

Abstract: We have studied a donor–acceptor fluorophore-labeled DNA switch where the acceptor is Alexa-647, a carbocyanine dye, in solution at the single molecule level to elucidate the fluorescence switching mechanism. The acceptor, which is in an initial high fluorescence trans state, undergoes a photoisomerization reaction resulting in two additional states during its sub-millisecond transit across the probe volume. These two states are assigned to a nonfluorescent triplet trans state that strongly quenches the donor emission and a singlet cis state that blocks the fluorescence resonance energy transfer (FRET) pathway and gives rise to donor-only fluorescence. The formation of these states is faster than the transit time, so that all three states are approximately equally populated under our experimental conditions. The acceptor dye can stick to the DNA in all these states, with the rate of unsticking determining the rate of isomerization into the other states. Measurement of the rate of change of the FRET signal therefore provides information about the fluorophore–DNA intramolecular dynamics. These results explain the large zero peak in the proximity ratio, often seen in single molecule FRET experiments, and suggest that photoinduced effects may be important in single molecule FRET experiments using carbocyanine dyes. They also suggest that for fast photoinduced switching the interactions of the acceptor dye with the DNA and other surfaces should be prevented.

Introduction

There is currently a great deal of interest in adapting biological molecules for new purposes. DNA has been used for a variety of new functions including molecular computation,¹ as a molecular motor,² as a scaffold for assembly,³ as a photonic wire,^{4,5} and as a single molecule optical switch.^{6–8} Some of these recent applications are based on the attachment of donor and acceptor fluorophores in close proximity on DNA where the acceptor fluorophore has been a carbocyanine dye, either

Cy5 or Alexa-647. Sauer and co-workers⁶ found that the DNA attached Cy5 dye, which has a trans conformation in the polymethine chain in its ground state, could act as a reversible single molecule switch. A structurally related dye Alexa-647 as shown in Figure 1 was also found to possess the same switching behavior.⁶ Measurements on a donor–acceptor system on immobilized DNA showed that the Cy5 could be converted into several nonfluorescent states, one that did not act as a FRET acceptor, and the other that appeared to be more strongly in resonance with the donor and acted as a better acceptor, which is probably the cis conformation.⁶ However it was not possible to determine the exact mechanism of the switching or the role of possible interactions between the Cy5 and the DNA from these experiments alone. Zhuang and co-workers⁸ also reported very recently a similar DNA-based reversible optical single molecule switch using a Cy3/Cy5 pair, and a steeper distance dependence between the two fluorophores than that in conventional FRET was found in experiments performed on surface-immobilized DNA. Again, the exact mechanism of the switching could not be determined. Similar fluorescence switching behavior in the DNA attached donor/acceptor system was also discovered by us, using the electric field generated inside the tip of a glass nanopipet rather than the optical method.⁷ In that experiment the DNA construct has Rhodamine Green as the donor and Alexa-647 as the acceptor. Here the switching

[†] Department of Chemistry, University of Cambridge.

[‡] Department of Physics and Astronomy, University College London.

- (1) For example, see: (a) Lipton, R. J. *Science* **1995**, *268*, 542–545. (b) Benenson, Y.; Gil, B.; Ben-Dor, U.; Adar, R.; Shapiro, E. *Nature* **2004**, *429*, 423–429.
- (2) For example, see: (a) Mao, C.; Sun, W.; Shen, Z.; Seeman, N. C. *Nature* **1999**, *397*, 144–146. (b) Yurke, B.; Turberfield, A. J.; Mills, A. P.; Simmel, F. C.; Neumann J. L. *Nature* **2000**, *406*, 605–608. (c) Yan, H.; Zhang, X.; Shen, Z.; Seeman, N. C. *Nature* **2002**, *415*, 62–65.
- (3) For example, see: (a) Seeman, N. C. *Nature* **2003**, *421*, 427–431. (b) Warner, M. G.; Hutchison, J. E. *Nat. Mater.* **2003**, *2*, 272–277. (c) Yan, H.; Park, S. H.; Finkelstein, G.; Reif, J. H.; LaBean, T. H. *Science* **2003**, *301*, 1882–1884.
- (4) Heilemann, M.; Tinnefeld, P.; Mosteiro, G. S.; Parajo, M. G.; Van Hulst, N. F.; Sauer, M. *J. Am. Chem. Soc.* **2004**, *126*, 6514–6515.
- (5) Vyawahare, S.; Eyal, S.; Mathews, K. D.; Quake S. R. *Nano Lett.* **2004**, *4*, 1035–1039.
- (6) Heilemann, M.; Margeat, E.; Kasper, R.; Sauer, M.; Tinnefeld, P. *J. Am. Chem. Soc.* **2005**, *127*, 3801–3806.
- (7) White, S. S.; Ying, L. M.; Balasubramanian, S.; Klenerman, D. *Angew. Chem., Int. Ed.* **2004**, *43*, 5926–5930.
- (8) Bates, M.; Blosser, T. R.; Zhuang, X. W. *Phys. Rev. Lett.* **2005**, *94*, art. no. 108101.

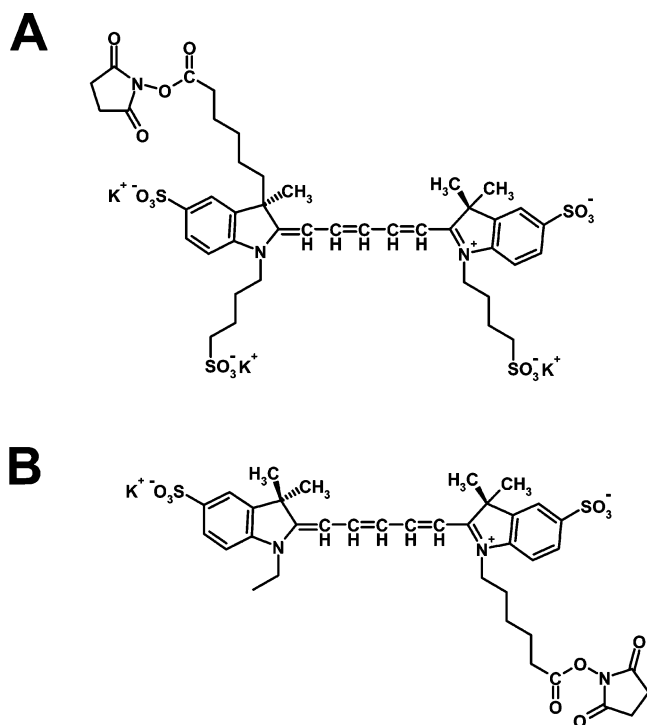


Figure 1. Structure of Alexa-647 dye¹⁰ (A) and cyanine 5 (B).

between donor-only fluorescence and acceptor-only fluorescence depends on the polarity of the electric field applied and occurred in less than 100 ms.⁷ The electric field driven optical switch, which is distinct from its optical driven counterpart, does not require oxygen removal and the addition of triplet quencher. Despite all these efforts, the mechanism which governs the fluorescence switching of single carbocyanine dyes is still elusive.

Motivated by these previous studies we have investigated a DNA-based molecular switch using Alexa-647 as an acceptor in solution at the single molecule level to obtain complementary information to the surface-based studies. We aimed to explore the link between fluorescence switching and dye–DNA interaction, to determine the rate at which the molecule could switch between donor-exclusive and acceptor-exclusive fluorescence, since our previous study using an electric field could only provide an upper limit of the rate of switching on the time scale of 100 ms, and to elucidate the mechanism of switching. This fundamental information may aid optimization of the switching effect for faster interconversion, which is important to the design of better single molecule optical switches, and clarify the potential complications arising from this switching behavior in single molecule experiments, particularly FRET-based measurements,⁹ using carbocyanine dyes.

Methods

DNA Samples. To make the overhang samples, an HPLC-purified 22-base oligonucleotide 5'-GCA CGT CGC AGC CGT CTA ATG U-3' was synthesized with a propargylamino-dU modified base at the 3' end (Transgenomic, U.K.). The 22-base oligonucleotide was desalted (NAP 5 column, Amersham, UK) and labeled with an Alexa Fluor 647 Oligonucleotide Amine Labeling Kit (Molecular Probes) following the manufacturer's instructions. The labeled oligonucleotide was separated from the excess dye using a Sephadex 25 (Amersham, UK) column

followed by ethanol precipitation and then from unlabeled DNA by gel electrophoresis. The bands containing labeled oligonucleotide were identified by visual inspection and UV shadowing. They were excised, and the DNA eluted into 10 mM Tris-HCl using the "crush and soak" method. The oligonucleotide was purified by extraction with phenol/chloroform/isoamyl alcohol 25:24:1, ethanol precipitation, and desalting with an NAP 5 column. An HPLC-purified 32-base, part-complementary oligonucleotide 5'-ATC GCG CCA TAC ATT AGA CGG CTG CGA CGT GC-3' was 5' labeled with tetramethylrhodamine (TMR) or Rhodamine Green (RG) via a 6-carbon linker; an unlabeled version was also synthesized for control fluorescence lifetime experiments (MWG-Biotech, Ebersberg, Germany (TMR and unlabeled), IBA GmbH, Germany (RG)). The 10-base "locking" oligonucleotide 5'-ATGGCGCGAT-3' was HPLC-purified and synthesized by MWG-Biotech, Ebersberg, Germany. All oligonucleotides were prepared in 10 mM Tris-HCl (Amersham, U.K.), 1 mM EDTA (Amersham, U.K.), 100 mM NaCl (Acros Organics, Fairlawn, NJ) pH 7.4 buffer solution. The concentration of the dye-labeled DNA was determined by UV-vis absorption at 260 nm, and the absorption at 505 nm (RG), 565 nm (TMR), or 650 nm (Alexa) was used as an internal reference. The double-stranded overhang sample was prepared by mixing the two complementary single-stranded oligonucleotides described above, heating to 90 °C, and slowly cooling to room temperature. It was found to have a melting temperature of 67 °C (in NaCl Tris EDTA buffer) using a UV-vis absorption spectrometer.

The same end and opposite end duplex DNA samples for the fluorescence lifetime experiments were prepared as previously described.⁷ Briefly HPLC-purified 40-base oligonucleotide 5'-TAG TGT AAC TTA AGC CTA GGA TAA GAG CCA GTA ATC GGT A-3' (MWG-Biotech, Ebersberg, Germany) was 3' labeled with the fluorophore Rhodamine Green (RG); a 5' RG labeled and unlabeled version were also purchased. Its 40-base complementary oligonucleotide with a 5' C6 amino modifier (IBA, Göttingen, Germany) was desalted (NAP 5 column, Amersham, U.K.) and labeled with an Alexa Fluor 647 Oligonucleotide Amine Labeling Kit (Molecular Probes, Eugene, OR).

Anisotropy Measurement. Steady-state fluorescence measurements were taken using an Aminco-Bowman Series 2 fluorimeter equipped with a water bath set to 20 °C, and a DNA concentration of 50 nM was used (and the locking strand at 500 nM where used). Fluorescence anisotropies for Rhodamine Green and Alexa 647 were calculated from the polarization of the emission components I_{VV} , I_{VH} , I_{HV} , and I_{HH} (where the subscripts denote the orientation of the excitation and emission polarizers) as $r = (I_{VV} - GI_{VH}) / (I_{VV} + 2GI_{VH})$, where $G = I_{HV} / I_{HH}$. For Rhodamine Green anisotropy, excitation was at 505 nm and emission was monitored at 530 nm. For Alexa 647, excitation was at 649 nm and emission monitored at 666 nm.

Single Molecule Measurement. The apparatus used to achieve single molecule fluorescence detection has been described in a recent publication.¹¹ Briefly a 514 or 488 nm laser beam from an argon ion laser (model 35LAP321–240, Melles Griot) was directed through a dichroic mirror and oil immersion objective (Apochromat 60×, NA 1.45, Nikon) to be focused 5 μm into a 1 mL sample solution supported in a Lab-TeK chambered coverglass (Scientific Laboratory Suppliers Ltd, U.K.).

Measurements were performed at a 50 pM overhang with or without 500 pM locking strand in 100 mM NaCl, 10 mM Tris-HCl, and 1 mM EDTA pH 7.4 buffer. All autocorrelation traces were taken with a bin time of 20 μs, and data were acquired for 3 min unless otherwise stated. To measure the proximity histogram a time bin of 1 ms was used and the data were acquired for 75 min.

The apparatus and experimental methods used to perform experiments in the nanopipet have been described previously.⁷ Briefly for

- (10) Terpetschnig, E. A.; Patsenker, L. D.; Tatarski, A. U.S. Patent Application No. 20040166515, August 26, 2004.
 (11) Li, H. T.; Ren, X. J.; Ying, L. M.; Balasubramanian, S.; Klenerman, D. *Proc. Natl. Acad. Sci. U.S.A.* **2004**, *101*, 14425–14430.

(9) Weiss, S. *Science* **1999**, *283*, 1676–1683.

the pipet experiments a 1 nM DNA solution was backfilled to the bent nanopipet by a microfiller (Microfil 34, World Precision Instruments, Sarasota, FL). A coverglass bottomed dish (Willco Wells GWST-1000) containing 2–3 mL of buffer was used as the bath. The pipet tip was placed 5 to 10 μm above the dish surface. Two Ag/AgCl electrodes, one in the bath and the other inside the pipet, served as the working and ground electrodes, respectively. The potential waveforms applied to the electrodes were created using a function generator (model DS345, Stanford Research Systems, Sunnyvale, CA). This function generator was also used to provide a trigger for the MCS cards.

The measurements of the proximity ratio histograms in the pipet and in solution were performed at room temperature, 20 $^{\circ}\text{C}$, with a 1 ms bin time used on both MCS cards. For the pipet experiment, a threshold of 35 counts per millisecond bin for the sum of the donor and acceptor fluorescence signals was used to differentiate background and single molecule bursts. A background of between 1 and 2 counts per millisecond, obtained from independent measurements of buffer solution without labeled DNA, was subtracted from each burst. For the solution experiment at different laser powers, a threshold of ~ 10 times the background was used, which ranges from 27 at 130 μW to 71 at 1400 μW .

Fluorescence Correlation Spectroscopy. We used the reference method and the proximity correlation method to determine intramolecular dynamics.¹¹ These methods are based on performing autocorrelation analysis of the donor fluorescence, I_D , or the proximity ratio, P , where

$$P = I_A / (I_A + I_D) \quad (1)$$

and I_A is the acceptor fluorescence. The autocorrelation function of I , where I is either I_D or P , was calculated using

$$G(\tau) = \frac{\langle \delta I(t) \delta I(t + \tau) \rangle}{\langle I(t) \rangle^2} \quad (2)$$

where $\langle I(t) \rangle$ is the time average of $I(t)$ and $\delta I(t)$ is the difference of $I(t)$ from $\langle I(t) \rangle$, the fluctuation in I . $\langle \delta I(t) \delta I(t + \tau) \rangle$ is the time average of the product of the fluctuation in I at time t and after a delay of $t + \tau$ and will only be nonzero within the time scale of the dynamics.

In the reference method, as described previously,¹¹ we measured the fluctuations of the donor fluorescence in time for the overhang sample with both donor and acceptor and in a separate experiment for a reference sample with donor only, where no FRET could occur. Fluctuations in donor fluorescence arise due to diffusion both in and out of the probe volume and due to intramolecular motion that changes the FRET efficiency. To eliminate the diffusional contribution the autocorrelation function of the donor and acceptor labeled overhang is divided by the autocorrelation function of the donor only. This autocorrelation function was then fitted with an exponential function.

The second method is based on measuring the fluctuations in the proximity ratio in time and forming the autocorrelation function. Fluctuations in the proximity ratio arise due to intramolecular motion; however since both donor and acceptor fluorophores are attached to the same molecule, the contribution of diffusion to the autocorrelation function is largely removed. The proximity correlation is filtered so that only proximity ratios in a certain selected range are correlated, by setting any proximity value outside the range to zero. This method is similar to filtered two-color ratiometric autocorrelation¹¹ and is performed in the single molecule limit. The autocorrelation functions were fitted using a stretched exponential

$$G_R(t) = G_R(0) \exp\left[-\left(\frac{t}{\tau}\right)^\beta\right] \quad (3)$$

where τ corresponds to the effective relaxation time associated with the correlated motion and β is a stretch parameter, describing the heterogeneity of the system. β can vary between 1 (where the system

displays normal two-state Arrhenius kinetics, with one discrete energy barrier) and 0 (where there is a continuum of equal energy barriers and the system shows power-law kinetics). The mean relaxation time $\langle \tau \rangle$ can be related to τ and β by

$$\langle \tau \rangle = \int_0^\infty \exp\left[-\left(\frac{t}{\tau}\right)^\beta\right] dt = \left(\frac{\tau}{\beta}\right) \Gamma(\beta^{-1}) \quad (4)$$

where $\Gamma(\beta^{-1})$ is a gamma function.

Fluorescence Lifetime Measurements. Measurements of fluorescence lifetime and anisotropy decays were undertaken using time-correlated single-photon counting (TCSPC) techniques which have been described in detail elsewhere.^{13,14} Fluorescence intensity and anisotropy decays were recorded for 100 nM concentrations of each sample in a 50 μL quartz fluorescence cuvette (Hellma) using a 90 $^{\circ}$ excitation-detection geometry. Excitation laser pulses at 488 nm were generated by an optical parametric amplifier (OPA 9000 Coherent) pumped at 250 kHz by a regeneratively amplified femtosecond Ti–Sapphire laser (Verdi V18, Mira900F, RegA9000, Coherent). The OPA pulses (c.a. 200 fs) were stretched to c.a. 1 ps by passage through a water cell and spectrally filtered by a 500 nm short pass interference filter (LS500 Corion) before focusing into the sample via a 10 cm focal length achromatic lens (Melles Griot) to a beam waist of about 15 μm . The excitation pulse energy and polarization was controlled using neutral density wheels, half waveplates, and linear polarizers (Opto-Sigma and Melles Griot). The powers used ranged from 0.6 μW to 5 μW to obtain a comparable peak count rate (c.a. 2.50 kHz). Higher powers between 5 and 110 μW were used for data taken with the streak camera due to its reduced sensitivity. The fluorescence was collected by a 5 cm aperture, 5 cm focal length lens (Melles Griot) and focused onto the microchannel plate photomultiplier (R3809U Hamamatsu). Scattered laser light was rejected, and donor fluorescence between 530 nm and 600 nm was selected using 515 and 530 nm glass filters (Schott) and a 600 nm short pass filter (LS600 Corion).

Fluorescence lifetime measurements were undertaken using an NIM-based TCSPC system (Ortec) with magic angle detection. Data collection times were approximately 35 min. A reference sample (buffer solution) was used to confirm the absence of any background fluorescence. Fast fluorescence decays were recorded over 1.1 ns using a high repetition rate streak camera (Hamamatsu C4334, instrument response fwhm 23.4 \pm 0.5 ps). For TCSPC anisotropy measurements excitation-fluorescence detection coincidence times were built up from alternating parallel and perpendicular fluorescence decays (10 s count window) using a rotating polarizer. The data collection time for each sample was approximately 25 min. TCSPC and streak camera lifetime analysis (deconvolution and fitting) was performed using FluoFit software (Picoquant).

Steady-State Quantum Yield. The steady-state quantum yield of the donor fluorophore (Rhodamine Green) for the different DNA samples was determined using Fluorescein (quantum yield 0.92 in 0.1 M NaOH) as a reference. Steady-state fluorescence measurements were taken using an Aminco-Bowman Series 2 fluorimeter, and a DNA (or Fluorescein in 0.1 M NaOH) concentration of 50 nM in 100 mM NaCl, 10 mM Tris-HCl, and 1 mM EDTA pH 7.4 buffer was used (and the locking strand at 500 nM where used). Both the DNA and Fluorescein samples were excited at the same wavelength (470 nm) and recorded with identical equipment parameters. The integrated area of the fluorescence emission spectra (S) and absorbance at 470 nm (A) are then used to calculate the quantum yield (ϕ) of Rhodamine Green using the following formula, $\phi_{\text{RG}} = S_{\text{RG}} \cdot \phi_{\text{F}} \cdot A_{\text{F}} / S_{\text{F}} \cdot A_{\text{RG}}$, where RG and F represent Rhodamine Green and Fluorescein, respectively.

- (12) Li, H. T.; Ying, L. M.; Green, J. J.; Balasubramanian, S.; Klenerman, D. *Anal. Chem.* **2003**, *75*, 1664–1670.
- (13) Bain, A. J.; Chandna, P.; Butcher, G. J. *Chem. Phys.* **2000**, *112*, 10435–10449.
- (14) Marsh, R.; Armoogum, D.; Bain, A. J. *Chem. Phys. Lett.* **2002**, *366*, 398–405.

DNA Overhang

5'-GCA CGT CGC AGC CGT CTA ATG U

3'-CGT GCA GCG TCG GCA GAT TAC ATA CCG CGC TA

DNA 'Locking Strand'

5'-AT GGC GCG AT

Figure 2. DNA overhang sequences used in this study. The donor is Rhodamine Green (green circle), and the acceptor is Alexa-647 (red circle). For experiments in the pipet, a Tetramethyl Rhodamine donor was used.

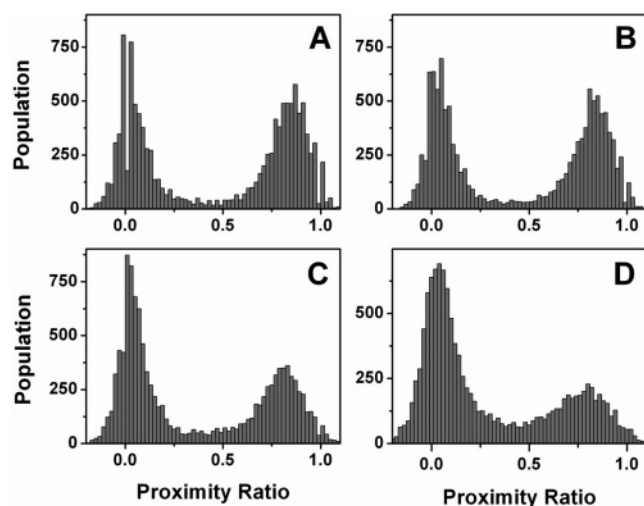


Figure 3. Variation of the proximity ratio histogram of the overhang sample with laser power. (A), (B), (C), and (D) were recorded with laser powers of 130, 210, 560, and 1400 μW , respectively.

Results and Discussion

DNA Overhang. We choose to study a DNA overhang sequence with a Rhodamine Green donor and Alexa-647 acceptor, as shown in Figure 2. This showed the same switching behavior as we have reported previously in the electric field in the pipet tip,⁷ but the fluorescence lifetime of its states turned out to be more easily resolvable using time-correlated single photon counting. In addition, the DNA sequence used can be made more rigid by adding a locking strand to bind to the overhang. This locking strand allows us to explore how much of any observed effects depend on the local environment of the fluorophore and how much depend on global DNA structure.

Anisotropy. The bulk anisotropy values for Rhodamine Green and Alexa-647 in the overhang alone were 0.165 ± 0.002 and 0.195 ± 0.003 , respectively, suggesting some interaction of both dyes with the DNA. The corresponding anisotropy values in the presence of the locking strand were similar, 0.160 ± 0.002 and 0.180 ± 0.003 for Rhodamine Green and Alexa-647, respectively.

Proximity Histograms in Solution. We first studied the power dependence of the proximity ratio histogram for the overhang sample. In these experiments it is necessary to increase the threshold used at higher powers due to the increased background and to keep the total number of single molecule events constant. The resulting threshold is close to 10 times the background. These data are shown in Figure 3.

At all powers, two subsets are clearly resolvable. These have peaks centered close to zero and 0.9, as we have reported

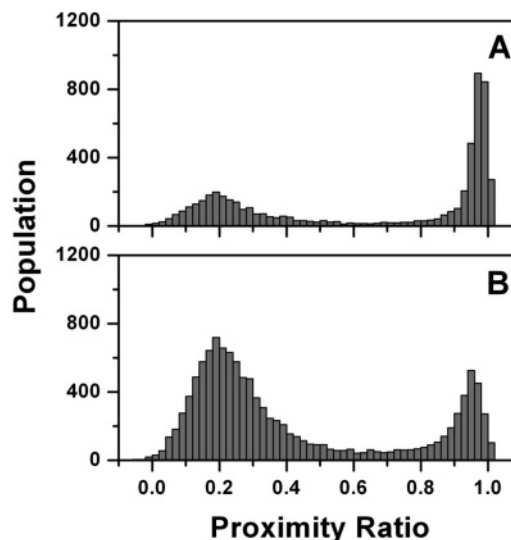


Figure 4. Effect of electric field on the single molecule FRET histograms of the DNA overhang (TMR version) in a nanopipet at 1 nM concentration upon excitation at 515 nm at the tip. (A) Positive potential (+1.0 V). (B) Slightly negative potential (−0.02 V).

previously.⁷ However the population of the high proximity ratio population decreases at higher power, and additional events are observed around 0.5. Following the recent single molecule analysis of Cy5 acceptor photobleaching by Seidel and co-workers,¹⁵ these changes in the histogram at higher laser powers, apparent above about 500 μW , are assigned to photobleaching. At the lowest powers used, where photobleaching is minimized, the relative populations of the low and high FRET peaks were 0.44 ± 0.06 and 0.56 ± 0.05 , respectively. Very similar histograms and relative populations were determined using the locking strand (data not shown).

The observation of two clearly distinguishable states for both the overhang and locked overhang at low powers means that these two states must interconvert on a significantly slower time scale than the mean diffusion time across the probe, 150 μs , or must interconvert by a third nonfluorescence state.

Electric Field Induced Switching in a Nanopipet. We studied the effect of applied potential on the population of the two states in the DNA overhang, with a Tetramethyl Rhodamine donor and an Alexa-647 acceptor, by using a nanopipet as described previously.⁷ As shown in Figure 4A, at a positive potential 43% of the population was in the low FRET state, and 57%, in the high FRET state. The overhang in free solution gave the same histogram (data not shown). On application of a negative potential there was 77% of the population in the low FRET state and only 23% in the high FRET state (Figure 4B). Thus the populations could be switched using the electric field in the pipet, although the overhang was not as effective a switch as the duplex DNA.

Dynamics. We then measured the intramolecular motion of the overhang and the overhang with a locking strand at low laser power, 30 μW in solution. Changes in the FRET histogram were only detectable at powers above 500 μW , so the power used for these dynamics experiments is an order of magnitude lower and hence any photobleaching contribution to the observed dynamics should be minimal. The first experiment was per-

(15) Eggeling, C.; Widengren, J.; Brand, L.; Schaffer, J.; Felekyan, S.; Seidel, C. A. M. *J. Phys. Chem. A* **2006**, *110*, 2979–2995.

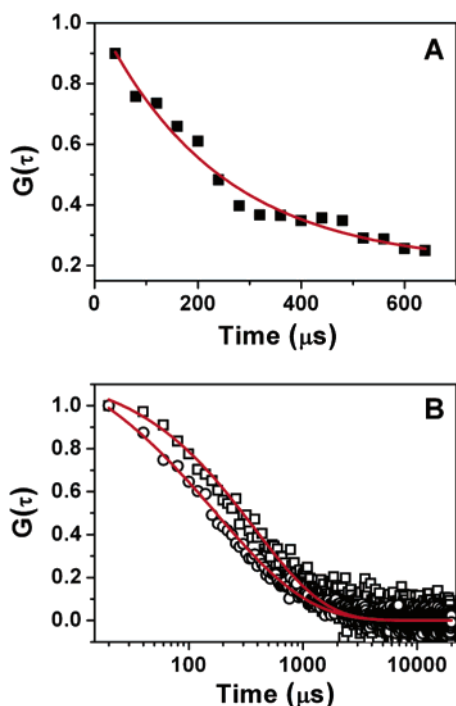


Figure 5. Fluorescence correlation measurements of the DNA overhang using (A) the reference method and (B) filtered proximity ratio correlation. In (B) \square and \circ represent low and high proximity ratio correlations, respectively.

formed at 10 nM, where there are on average 10 molecules in the probe volume at any one time so that the rate measured is the sum of all the intramolecular motions (Figure 5A) using the reference method (see Methods for details). This gave an average time of 235 μs and 310 μs for the intramolecular motion of the overhang and the overhang with the locking strand, respectively.

We then applied the filtered proximity correlation in the single molecule limit by only correlating proximity ratios in the range $0 \leq P \leq 0.5$ for the low proximity peak and $0.5 < P \leq 1$ for the high peak. The high proximity ratio subpopulation and low proximity ratio subpopulation gave different time constants for their autocorrelation functions as shown in Figure 5B. For the overhang the high proximity subpopulation gave a mean time of 270 and 350 μs for the overhang and the overhang with the locking strand, respectively. The low proximity subpopulation gave a mean time of 450 and 700 μs for the overhang and the overhang with the locking strand, respectively. The β value was close to 0.4 in all cases. A β value of 0.4 suggests that there might be several parallel pathways that the fluorophore can leave the high or low proximity state. A temperature dependence study showed no detectable variation in mean time with temperature suggesting a low barrier to interconversion between conformations (data not shown). The results are summarized in Table 1.

Note that the reference method measures the rate of all intramolecular motions. In these experiments, the filtered proximity ratio method (FPRM) just measures the rate the molecule leaves the low or high proximity state. The calculated overall rate from FPRM is $(454^{-1} + 277^{-1})^{-1} \mu\text{s}$, i.e., 172 μs , for the overhang and $(704^{-1} + 353^{-1})^{-1}$, i.e., 235 μs , with the locking strand in reasonable agreement, within 30%, with the reference method. The FPRM method shows that the rate of motion is faster from the high proximity state than from the

Table 1. Mean Time for Intramolecular Motion and Beta Parameter Obtained Using the Reference Method and Filtered Proximity Ratio Method for the DNA Overhang and Locked DNA Overhang (See Text for Details)

	$\langle T \rangle (\mu\text{s})$	β
reference method (10 nM)	234 \pm 34	1 (fixed)
reference method locking (10 nM)	311 \pm 18	1 (fixed)
filtered proximity ratio overhang (low P)	454 \pm 36	0.42 \pm 0.03
filtered proximity ratio overhang (high P)	277 \pm 15	0.46 \pm 0.02
filtered proximity ratio overhang + locking (low P)	704 \pm 12	0.44 \pm 0.02
filtered proximity ratio overhang + locking (high P)	353 \pm 27	0.45 \pm 0.03

low proximity state and both rates increase in approximate proportion on addition of the locking strand. This dependence on the locking strand suggests that the measured rates depend on the DNA structure and do not solely depend on local motion of the fluorophore on its linker.

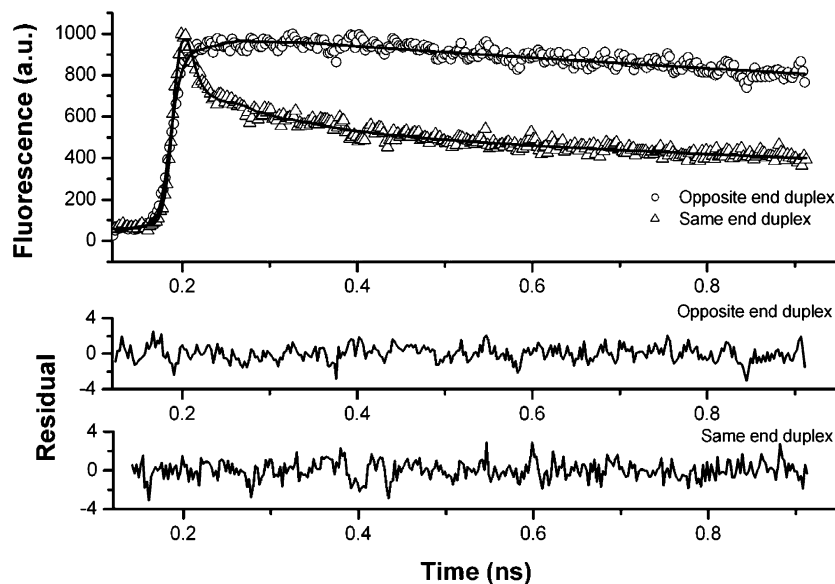
Importantly, we have found that the mean times for intramolecular motion are only a factor of 2–5 longer than the mean diffusion time. This indicates that the low proximity peak cannot interconvert directly with the high proximity peak but must do so via a third dark state, not detectable by fluorescence.

Fluorescence Lifetime. We then performed ensemble fluorescence lifetime measurements of the donor fluorophore, detecting fluorescence between 530 nm and 600 nm, to get direct evidence for the suggested dark state. The different states of the acceptor would result in different fluorescence donor lifetimes, since each acceptor state would have a different FRET efficiency. We also measured the fluorescence lifetimes of the duplex DNA that we have studied previously with the donor and acceptor at the same end or opposite ends for comparison.⁷ The results are summarized in Table 2.

The fluorescence lifetime of Rhodamine Green in solution is 4.3 ns. The donor-only overhang is fitted with two lifetimes, one due to free dye (81.5%) and one due to quenching of the donor (18.5%) by interaction with the DNA. When this overhang is locked, then interactions of the donor with the DNA are reduced so that the amplitude of this quenched lifetime is also reduced to 7%. The opposite end duplex has negligible FRET and also shows two lifetimes, one due to free dye and one quenched due to the interaction with the DNA of similar time constants and amplitudes. For the overhang with both donor and acceptor present, FRET between the donor and acceptor was also possible, and it was necessary to fit with three lifetimes as judged by the values of reduced chi-square. Without the locking strand there was a population with a lifetime close to 4 ns, one with a lifetime of 1.3 ns and a third lifetime of 0.33 ns. The lifetime at 3.8 ns is due to the free dye providing additional evidence for the acceptor existing in a state that does not FRET with the donor. The reduction in lifetime from 3.8 to 0.33 ns is due to FRET with the acceptor giving an estimated FRET efficiency of 0.9 in good agreement with the single molecule histogram. The lifetime at 1.3 ns corresponds to a quenched state of the donor, due to interaction with the DNA, which is also present in the donor-only overhang. Addition of the locking strand makes the FRET efficiency decrease slightly (due to the increase in donor–acceptor distance on formation of duplex

Table 2. Fluorescence Lifetimes and Quantum Yields of Donor Fluorophores on Duplex DNA, Overhang DNA, and Locked Overhang DNA

DNA	T_1 (ns)	A_1 (%)	T_2 (ns)	A_2 (%)	T_3 (ns)	A_3 (%)	χ^2	quantum yield
overhang (D)	3.79 ± 0.02	81.5 ± 0.1	1.4 ± 0.1	18.5 ± 0.4			1.53	0.31
locked overhang (D)	4.75 ± 0.02	92.9 ± 0.2	1.2 ± 0.3	7.1 ± 0.5			1.65	0.75
overhang (D + A)	3.80 ± 0.03	35.8 ± 0.1	1.3 ± 0.1	32.1 ± 0.2	0.33 ± 0.06	32.1 ± 1.0	1.39	0.18
locked overhang (D + A)	4.58 ± 0.06	34.0 ± 0.1	1.5 ± 0.2	38.2 ± 0.2	0.50 ± 0.10	27.8 ± 0.7	1.56	0.41
opposite end duplex (D + A)	4.47 ± 0.03	84.4 ± 0.2	1.5 ± 0.1	15.6 ± 0.4			1.38	0.64
same end duplex (D + A)	3.94 ± 0.03	40.2 ± 0.1	1.5 ± 0.1	14.6 ± 0.1	0.12 ± 0.01	45.2 ± 1.6	1.22	0.20

**Figure 6.** Streak camera measurements of the fluorescence decays of the same end and opposite end duplex DNA with donor and acceptor taken with a pulse energy of 440 pJ. The solid lines show the fits to the decays.

DNA) so that the lifetime of the shortest FRET state increases to 0.5 ns. When both fluorophores are at the same end of the duplex DNA, FRET should now be highly efficient, and we see a decrease in the lifetime of the state due to FRET to 0.12 ns corresponding to an FRET efficiency of 0.97.

The quantum yields were also measured in a steady-state experiment. The locked overhang quantum yield is more than double that of the overhang which indicates that there are also other donor dark states for the overhang whose lifetimes are too short to be detected in our time-resolved experiments (the instrument response function is c.a. 67 ps) probably due to increased interactions of the dye with the flexible DNA in the overhang. Addition of an acceptor to the overhang gives the expected reduction in donor quantum yields due to FRET. When the overhang is locked, the environment of the donor changes so that quenching interactions are reduced and the quantum yield increases. On addition of an acceptor to the locked overhang, there is still a clear reduction in quantum yield of the donor in the presence of the acceptor due to FRET. The opposite end duplex has a high quantum yield, similar to the locked overhang, while the same end duplex quantum yield is reduced by a factor of 4 due to efficient FRET.

These experiments in combination show clear evidence for FRET between the donor and acceptor in the DNA constructs and an additional donor state that does not FRET with the acceptor. They provide no evidence for an additional dark quenching state of the acceptor which can efficiently FRET with the donor. We therefore performed an experiment with a higher time resolution on the same end and opposite end duplex DNA

with donor and acceptor dyes, where there is no evidence of additional dark donor states. FRET and consequential excitation of the acceptor only occurs when donor and acceptor are at the same end of the duplex. These experiments were performed with a streak camera with an instrument response function of 23 ps. As shown in Figure 6, this experiment at a 440 pJ pulse energy resolved the fast component for the same end duplex previously measured to be 120 ps into two lifetimes: one of 6.1 ± 0.3 ps and one of 89.9 ± 0.7 ps with amplitudes of $78 \pm 5\%$ and $7.5 \pm 0.5\%$, respectively. In contrast, as shown in Figure 6, the opposite end duplex did not show these fast decays. The amplitude and lifetime of the fast component of the same end duplex were found dependent on the laser pulse power, possibly due to direct excitation of the acceptor, so a power dependence study was performed from a pulse energy of 80 pJ down to 20 pJ, the lowest power with which it was possible to take data with adequate signal-to-noise. The result of a global fit of these data is shown in Table 3. The lifetime of the fast component is 18 ps and its amplitude is $\sim 50\%$, while the other component has a lifetime of ~ 110 ps with an amplitude of $\sim 10\%$. These results show that, as well as efficient FRET between the donor and acceptor giving rise to the state with a lifetime of 110 ps, there is a significant population of an additional heavily quenching state of the acceptor present, reducing the donor lifetime to 18 ps.

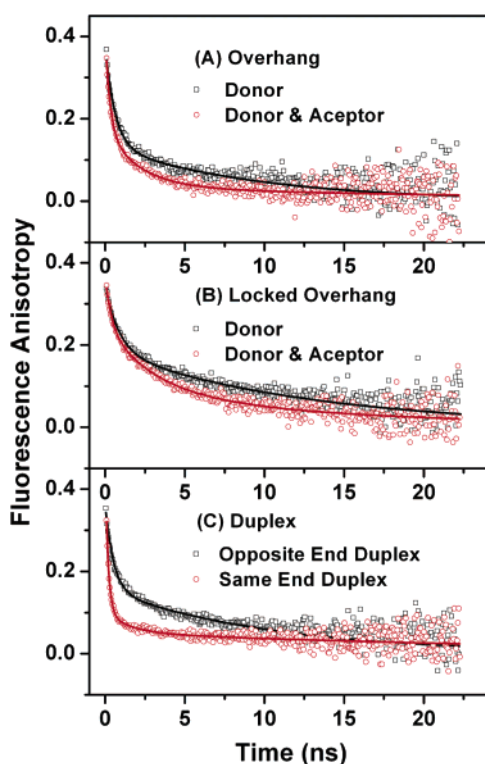
Fluorescence Anisotropy. The results of the fluorescence anisotropy measurements are summarized in Table 4, and the decays are shown in Figure 7. The data for constructs with donor-only and the opposite end duplex, which has no FRET,

Table 3. Global Fit to Streak Camera Data for the Same End Duplex Taken with 20–80 pJ Pulse Energy

DNA	T_1 (ns)	A_1 (%)	T_2 (ns)	A_2 (%)	T_3 (ns)	A_3 (%)	T_4 (ps)	A_4 (%)	χ^2
same end duplex (D + A) 80 pJ	3.94 (fixed)	18.6 ± 1.00	1.48 (fixed)	11.3 ± 1.2	0.11 ± 0.02	8.7 ± 4.7	18.1 ± 2.3	61.3 ± 17.1	1.095
same end duplex (D + A) 40 pJ	3.94 (fixed)	23.0 ± 0.9	1.481 (fixed)	11.0 ± 1	0.11 ± 0.02	9.4 ± 4.1	18.1 ± 2.3	56.6 ± 14.3	1.074
same end duplex (D + A) 20 pJ	3.94 (fixed)	23.7 ± 0.5	1.48 (fixed)	12.0 ± 0.5	0.11 ± 0.02	10.8 ± 2.2	18.1 ± 2.3	53.5 ± 7.6	0.976

Table 4. Fluorescence Anisotropy Measurements of Donor Fluorophores of Donor Fluorophores on Overhang DNA, Locked Overhang DNA, and Duplex DNA

DNA	T_1 (ns)	A_1 (%)	T_2 (ns)	A_2 (%)	T_3 (ns)	A_3 (%)	cone angle (deg)	χ^2
overhang (D)			0.67 ± 0.02	63.6 ± 0.9	9.3 ± 0.3	36.4 ± 0.7	46.4 ± 0.4	1.39
locked overhang (D)			0.96 ± 0.04	44.9 ± 0.9	12.7 ± 0.3	55.1 ± 0.8	39.4 ± 0.3	1.23
overhang (D+A)	0.30 ± 0.01	56 ± 2	2.1 ± 0.3	35 ± 2	27 ± 15	8 ± 2		1.07
locked overhang (D + A)	0.38 ± 0.04	28 ± 2	3.1 ± 0.5	41 ± 5	16 ± 5	21 ± 6		0.99
opposite end duplex (D + A)			0.55 ± 0.02	56.5 ± 0.7	10.4 ± 0.2	43.5 ± 0.5	43.2 ± 0.2	1.49
same end duplex (D + A)	0.18 ± 0.01	76 ± 2	1.4 ± 0.2	12 ± 1	29 ± 5	12 ± 1		1.09

**Figure 7.** Fluorescence anisotropy decays for (A) the overhang, (B) the locked overhang, and (C) duplex DNA constructs. The black squares indicate the anisotropy decays for the donor in the absence of the acceptor or for (C) where no FRET is possible due to the distance between donor and acceptor. The red circles are for the constructs where both donor and acceptor are present and are close enough for efficient FRET.

were fitted with two exponential decays and an initial anisotropy, $R(0)$. For constructs where donor and acceptor were in close proximity, a third exponential was required to fit the data. The cone model of Kinosita et al.¹⁶ has been widely used to interpret

the fluorescence anisotropy of noninteracting molecular probes within macromolecules. Restricted rotational diffusion is modeled as diffusion or “wobbling” confined to a cone defined by the angular limits $0 \leq \theta \leq \theta_{\max}$, where θ_{\max} is the maximum angle of the cone. The anisotropy decay is then approximately biexponential with a slow overall isotropic diffusion (T_3) moderating a faster restricted rotational local diffusion (T_2). The change in anisotropy with time, $R(t)$, is given by

$$R(t) = R(0) \exp(-t/T_3)[A_3 + A_2 \exp(-t/T_2)] \quad (5)$$

From ref 16 the cone angle is given by

$$\sqrt{A_3} = \frac{1}{2}[\cos \theta_{\max}(1 + \cos \theta_{\max})] \quad (6)$$

Using this approach, the fluorescence anisotropy decays of the donor in the absence of FRET could be modeled as restricted local rotational motion (T_2 c.a. 0.5–1.0 ns) within a cone (θ_{\max} c.a. 39° – 46°) mediated by the slower diffusion of DNA (T_3 c.a. 9–13 ns). In the presence of FRET, the fluorescence anisotropy ($R_{\text{FRET}}(t)$) is modified by an additional fast (c.a. 180–380 ps) depolarization component (T_1):

$$R_{\text{FRET}}(t) = R(0)[A_1 \exp(-t/T_1) + A_2 \exp(-t/T_2) + A_3 \exp(-t/T_3)] \quad (7)$$

In fixed interacting systems depolarization of the donor anisotropy due to FRET is forbidden.¹⁷ However, theoretical models of Tanaka¹⁸ indicate that the donor anisotropy can itself be depolarized as a result of FRET if the relative orientations of the two species are time-dependent as, for example, a result of local rotational diffusion of either species within the DNA host. Indeed, for all three constructs where FRET is expected the depolarization of the donor is faster and more marked; this can be seen in Figure 7 where the donor fluorescence anisotropy

(16) Kinosita, K.; Kawato, S.; Ikagami, A. *Biophys. J.* **1977**, *20*, 289–305.

(17) Tanaka, F.; Mataga, N. *Photochem. Photobiol.* **1979**, *29*, 1091–1097.

(18) Tanaka, F. *J. Chem. Phys.* **1998**, *109*, 1084–1092.

pies for equivalent constructs are compared. These observations are most striking in the case of the same end duplex construct where the amplitude of the fast (c.a. 180 ps) depolarization component of the anisotropy A_1 is significantly larger than A_2 for the opposite end construct due to efficient FRET in good agreement with the lifetime measurements.

Discussion

Alexa-647 exists in three states. The FRET histograms we observed would be expected to show a single peak, since it is expected that the DNA exists in a single conformation or a range of conformations with the same average FRET efficiency. However we have observed two clear peaks in the proximity ratio histogram, one at high proximity ratio corresponding to efficient energy transfer and one at low proximity ratio corresponding to very inefficient energy transfer. If there was direct conversion between these two states on the time scale of the diffusion time across the probe volume, then this would result in one broad peak. However we have also measured rates for the disappearance from these two states that are comparable to the diffusion time for the molecule across the probe volume. This is only possible if the Alexa-647 does not convert directly between the high and low proximity states but goes via a third state which is nonfluorescent and also results in no donor fluorescence; i.e., it is totally dark. This would need to be a state where there is efficient energy transfer but the acceptor is nonfluorescent and, hence, acts as a quencher. We have also found independent evidence for three acceptor states from the ensemble fluorescence lifetime measurements of the donor taken with the streak camera. In the single molecule experiments these three states of the Alexa-647 are formed rapidly during the molecule's transit across the probe volume, since the dye exists only in the trans form in its ground state.

These three states are likely to be isomers with different photophysical properties formed by photoreactions when the acceptor is in its excited state. It is known that cyanine dyes exist only in the trans state in their ground state.¹⁹ Schwille and co-workers found that Cy5 dye could photoisomerize fast to the cis form in 40–200 ns and also photoisomerize back to the trans form in its excited state.²⁰ The cis state will have a different absorption spectrum, and this has recently been measured for Cy5. The results of recent transient absorption experiments²¹ showed that the cis state is red shifted to a peak at 690 nm, compared to the trans state at 650 nm. This has two consequences: first the cis state has a much poorer overlap with the donor emission spectrum and hence the FRET efficiency will be less; second, the interconversion from the ground state cis to trans, via excited-state photoisomerization, is slow on the time scale of our experiment due to poor excitation of the cis excited state. Hence we observe two distinct peaks in the proximity ratio histograms. This assumes Alexa-647 shows the same red-shift in its cis state as Cy5 which seems likely based on the structural similarities of the dyes and their similar absorption and emission spectra. We therefore assign the low proximity ratio peak to *cis*-Alexa-647.

The dark state must also be formed by a photoreaction since it is formed rapidly. One possibility is a second photoisomer-

ization reaction to produce a *cis*–*cis* state. Work by Batyuto et al.²² demonstrates that dibcarbocyanine dyes show stepwise photoisomerization to form a *cis* and $\gamma\beta$ di-*cis* product. The shift in the absorption spectrum is in the opposite direction for the two isomers and depends on the electron-donor ability of terminal groups. Similar evidence has been found for the photoisomerization of DTDCI cyanine dye by Vaveliuk et al.²³ where two photoisomers were observed. The first isomer had a strongly overlapped absorption spectrum with the normal species, and the second isomer, a red-shifted spectrum. Based on these studies we could assign the dark state to a *cis*–*cis* state that had better overlap with the donor fluorescence spectrum and hence would act as an effective quencher producing a dark state. However, a more recent transient absorption study of Cy5²¹ has provided more convincing evidence for this dark state being a trans triplet state. A peak was found at 625 nm on top of the ground-state absorption of the trans form.²¹ Based on the increased absorption in the presence of a triplet promoter, this state is assigned to the trans triplet state of Cy5. As suggested in this recent study,²⁰ this state would be effectively excited by FRET to a higher triplet state, due to good overlap between donor emission and the absorption spectrum of the trans triplet state, and returns to the ground state by a variety of nonfluorescent pathways, producing a dark state. The only state via which it is not possible to return is the trans S_1 state since this will result in fluorescence, but the *cis* T_1 and S_1 and trans T_1 are all possibilities. Thus the dark state is one isomer of dye that has efficient FRET with the donor but is nonfluorescent, and based on the most recent work,^{21,24} this would be assigned to the trans T_1 state of Alexa-647. The key states assumed to be involved are shown in Figure 8.

The transient absorption experiments on Cy5 were performed in deoxygenated ethanol so the triplet state will be significantly longer lived than in our experiments where oxygen is present. This difference and the different solvents mean that we cannot use the rates from the transient absorption experiment to estimate rates for the photoreactions in our experiments. However, qualitatively the fast photoisomerization and back-reaction in the S_1 state would result in an equilibrium between trans S_1 and *cis* S_1 being rapidly reached. The ratio of fraction of molecules in the ground state trans S_0 and *cis* S_0 states will reflect this equilibrium. A second equilibrium would also be rapidly set up with the trans T_1 state, due to fast intersystem crossing taking about 1 μ s.²⁰ Both the isomerization pathway from the trans S_1 state to the *cis* T_1 state and the back-isomerization from the *cis* T_1 state to the trans S_1 state shown in Figure 8 have been observed.^{21,24} It was also suggested that the potential energy surfaces of *cis* T_1 and trans S_1 are almost degenerate.²⁴ Taking these factors into account, we would expect that all four states would be involved in the photophysics of the chromophore and significantly populated. It should also be

(19) Baraldi, I.; Carnevali, A.; Momicchioli, F.; Ponterini, G. *Spectrochim. Acta A* **1993**, *49*, 471–495.

(20) Widengren, J.; Schwille, P. *J. Phys. Chem. A* **2000**, *104*, 6416–6428.

(21) Huang, Z. X.; Ji, D. M.; Wang, S. F.; Xia, A. D.; Koberling, F.; Patting, M.; Erdmann, R. *J. Phys. Chem. A* **2006**, *110*, 45–50.

(22) Batyuto, Y. V.; Razumova, T. K.; Tarnovskii, A. N. *Opt. Spectrosc.* **2002**, *93*, 399–407.

(23) Vaveliuk, P.; Scaffardi, L. B.; Duchowicz, R. *J. Phys. Chem.* **1996**, *100*, 11630–11635.

(24) Huang, Z. X.; Ji, D. M.; Wang, S. F.; Xia, A. D.; Koberling, F.; Patting, M.; Erdmann, R. *J. Am. Chem. Soc.* **2005**, *127*, 8064–8066.

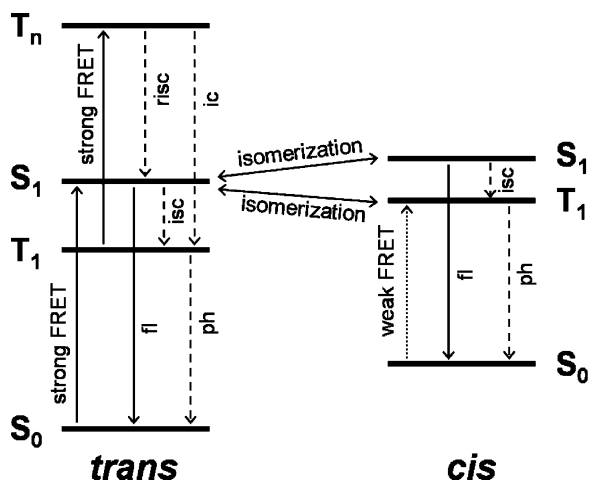


Figure 8. Schematic of energy levels of trans and cis states involved in the FRET mediated photoisomerization and back-isomerization. S_0 , S_1 , T_1 , and T_n represent the ground singlet, excited singlet, first triplet, and excited triplet states of Alexa-647 dye, respectively. Abbreviations fl, ph, isc, risc, and ic denote fluorescence, phosphorescence, intersystem crossing, reverse intersystem crossing, and internal conversion, respectively. The scheme shows major processes only.

noted that the cis T_1 state also absorbs around 690 nm; therefore this state may contribute to the low or “zero” FRET peak as well.

Dynamics. There has been a detailed study of FRET-mediated acceptor excitation by Seidel and co-workers using fluorescence correlation spectroscopy.²⁵ This study shows that for duplex DNA with a Cy5 acceptor at one end the measured isomerization rate (the sum of the forward and backward isomerization rates) depends linearly on laser power and increases with the FRET efficiency. This study determined the rate constant for crossing from the trans excited-state S_1 to the triplet to be $0.5 \times 10^6 \text{ s}^{-1}$ and the rate constant for deactivation of the triplet state to be $0.2 \times 10^6 \text{ s}^{-1}$, in agreement with previous measurements on DNA.²⁰ Both studies^{20,25} showed that the isomerization rate of Cy5 was reduced by a factor of 5 compared to the free dye. This reduction indicates a change in local viscosity when the dye is attached to the DNA. The question then arises what are the time constants that we are measuring in our experiment? Do they report back about photoisomerization rates of the acceptor or about intramolecular motion of the acceptor which is attached to the DNA?

The easiest way to address this question is to estimate the overall isomerization rate, the sum of the forward and backward isomerization rates, at our excitation intensity, 14 kW cm^{-2} (excitation power $30 \mu\text{W}$ focused to a beam waist of 260 nm measured by fluorescence correlation of Rhodamine 6G in solution). For the highest FRET DNA sample with a four base pair separation between donor and acceptor studied previously,²⁵ the linear plot with power has a gradient of $8.2 \text{ ms}^{-1}/\text{kW cm}^{-2}$. This study showed that the isomerization rate is reduced by a factor of 5 compared to the free dye. So at our laser intensity the estimated overall isomerization rate would be $1.2 \times 10^5 \text{ s}^{-1}$, giving a lifetime of $\sim 9 \mu\text{s}$. A more recent measurement of Cy5 photoisomerization on a hairpin DNA gave a rate constant of $(1-2) \times 10^4 \text{ s}^{-1}$ at an excitation intensity of $(0.5-1) \text{ kW/}$

cm^2 ,²⁶ which would give a slightly faster isomerization rate of $\sim 3 \times 10^5 \text{ s}^{-1}$ with a 14 kW/cm^2 excitation intensity. The mean relaxation times we have measured using the reference method and proximity ratio filtered autocorrelation are significantly slower, by a factor of 20 compared to the dye on a DNA construct in ref 24 and 100 compared to the free dye. The rate of crossing to the triplet state for Cy5 is also much faster (time constant $\sim 1 \mu\text{s}$).²⁰ While there may be some differences in photophysics between Alexa-647 and Cy5, based on their similarity in structure this is unlikely. We therefore cannot be measuring crossing to the triplet state or photoisomerization in our experiment since they would lead to a single broad peak in the proximity histogram. It is more likely that the reason that measured rates are so much slower with the dye attached to DNA is due to the isomers sticking to the DNA as suggested by Sauer.⁶ Once stuck to the DNA the photoisomerization rate is significantly reduced, or not possible, so that the dye needs to unstuck before fast photoisomerization can occur. Some fraction of the dye is effectively trapped in each photoisomer state by sticking to the DNA, since the time taken to unstuck is longer than the average transit time across the probe volume. It is the unsticking rates that we measure. The rates for unsticking for the trans and cis states are within a factor of 2 of each other, as would be expected for isomers of the same molecule. This sticking would not involve strong bond formation, but rather weak noncovalent interactions where the loss of entropy on binding to DNA is compensated by a gain in enthalpy, and hence there would be no measurable activation barrier as we have found in our temperature-dependent studies (data not shown). Locking of the overhang produces no large change in the population of the three states as measured by the fluorescence lifetime, in agreement with the FRET histograms. We note that interaction or sticking of fluorophores to DNA has also been observed in other single molecule experiments on a comparable time scale.^{25,27}

The unstuck dye can photoisomerize fast and set up the photoequilibrium as described above, giving rise to approximately equal populations of the low FRET, high FRET, and dark state. Some fraction of these different isomers is then trapped by sticking to the DNA, and the unsticking rate, which is the intramolecular motion of the fluorophore on the DNA, is measured in our experiment. Therefore, our experiments indicate that, despite the photoinduced isomerization of Alexa-647 occurring at low laser power, we probe the dynamics of the intramolecular motion of the fluorophore.

Single Molecule Switching. We will now consider if this model is in agreement with previous data on single molecule switching. Qualitatively our model is consistent with that proposed by Sauer and co-workers⁶ in that switching involves formation of a cis state and also sticking of the fluorophore to the DNA. However quantitatively there is a difference in measured rates between solution phase and surface immobilization studies. Slower rates, on the order of a few milliseconds, were observed in surface studies. This may reflect differences in experimental conditions since the surface experiments were performed under conditions of oxygen removal and addition of

(25) Widengren, J.; Schweinberger, E.; Berger, S.; Seidel, C. A. M. *J. Phys. Chem. A* **2001**, *105*, 6851–6866.

(26) Cosa, G.; Harbron, E. J.; Zeng, Y. N.; Liu, H. W.; O'Connor, D. B.; Eta-Hosokawa, C.; Musier-Forsyth, K.; Barbara, P. F. *Biophys. J.* **2004**, *87*, 2759–2767.

(27) Edman, L.; Mets, U.; Rigler, R. *Proc. Natl. Acad. Sci. U.S.A.* **1996**, *93*, 6710–6715.

a triplet quencher. They may also simply be due to structural differences between the two fluorophores or differences in the local microenvironment of the fluorophores due to differences in the local DNA structure. However, surface constraints and steric hindrance may also affect the photophysics of the dye, just as we have observed that sticking of the dye to the DNA reduces the photoisomerization rate. There is also evidence that surface attachment can alter the dynamics and accessible conformations of DNA,^{28,29} although this will depend on the surface chemistry used. This may mean that the dye spends a longer time stuck to the DNA or surface before it unsticks and can photoisomerize. In addition, it is also possible that steric constraints affect which double bond undergoes photoisomerization and the rate of photoisomerization.³⁰ Therefore the rates of many of the competing processes shown in Figure 8 seem likely to depend on the local microenvironment of the fluorophore and hence depend on the DNA sequence, local oxygen concentration, presence of triplet quencher or intersystem crossing enhancer, and steric hindrance due to the fluorophore sticking to the DNA or surface making quantitative comparisons more difficult.

In the presence of a strong electric field⁷ the potential energy surface for photoisomerization may be altered making one of the excited state trans or cis forms more stable. Depending on the polarity and magnitude of the field, fluorophores may be pushed into either the high FRET trans states or the low FRET cis states. Our study shows that switching rates of less than 1 ms are possible in the absence of an electric field and that if sticking to the DNA is prevented switching rates less than 1 μ s may be possible.

Conclusions

We have studied a single molecule switch in free solution eliminating any possible surface effects. Molecule-by-molecule analysis has allowed us to identify the different fluorescence states of the acceptor and their dynamics. To do this we have used the filtered proximity ratio autocorrelation to determine the rate for intramolecular motion from one substate of the molecule, and this is key to elucidating the mechanism of the

switching process, since it showed that the switching must go through a third dark state. Photoisomerization gives rise to a form of the Alexa-647 dye that has poor energy transfer with the donor fluorophore, assigned to a cis state, and this gives rise to a significant donor peak in the proximity histogram as has been observed previously for single molecule FRET studies using Cy5.³¹ The dependence of histograms on power means that the real distance between donor and acceptor could not be determined, unless the measurement is carried out at such a low power that any photophysical effect is negligible. These results are important for single molecule FRET studies. While histograms are affected, the dynamics measured here is still the motion of the fluorophore and not the rate of photoisomerization. This is probably the case in other studies using Cy5. It may be desirable to prevent dye–DNA interaction for single molecule experiments to make interpretation of data simpler, or alternatively it may be better to use the dye locked in the trans form.

Our results show that the single molecule DNA photoswitch exists in three states, that switching can take place in less than a millisecond, and that one needs to prevent sticking to the DNA for faster switching. This may be possible by optimization of the linker between the nucleotide and the fluorophore or use of different DNA constructs where the fluorophore interacts less strongly with the DNA. Higher laser powers would also increase the rate of switching. Conversely if one wants to trap the switch in one state it is necessary to hinder the isomerization or the switched state needs to have a significant change in its absorption spectrum, so that once switched it is no longer effectively excited. If these conditions can be met then fast controlled molecular photoswitching should then become feasible with possible applications in areas such as bioimaging and information storage.^{32–34}

Acknowledgment. We thank the BBSRC and EPSRC for funding. We also thank Angel Orte for proofreading the manuscript.

JA0614870

(28) Grunwell, J. R.; Glass, J. L.; Lacoste, T. D.; Deniz, A. A.; Chemla, D. S.; Schultz, P. G. *J. Am. Chem. Soc.* **2001**, *123*, 4295–4303.

(29) Osborne, M. A.; Barnes, C. L.; Balasubramanian, S.; Klenerman, D. *J. Phys. Chem. B* **2001**, *105*, 3120–3126.

(30) Benniston, A. C.; Harriman, A.; McAvoy, C. *J. Chem. Soc., Faraday Trans.* **1997**, *93*, 3653–3662.

(31) Deniz, A. A.; Dahan, M.; Grunwell, J. R.; Ha, T. J.; Faulhaber, A. E.; Chemla, D. S.; Weiss, S.; Schultz, P. G. *Proc. Natl. Acad. Sci. U.S.A.* **1999**, *96*, 3670–3675.

(32) Vogt, G.; Krampert, G.; Niklaus, P.; Nuernberger, P.; Gerber, G. *Phys. Rev. Lett.* **2005**, *94*, art. no. 068305.

(33) Habuchi, S.; Ando, R.; Dedecker, P.; Verheijen, W.; Mizuno, H.; Miyawaki, A.; Hofkens, J. *Proc. Natl. Acad. Sci. U.S.A.* **2005**, *102*, 9511–9516.

(34) Sauer, M. *Proc. Natl. Acad. Sci. U.S.A.* **2005**, *102*, 9433–9434.